Journal of Fluorescence (2019) 29:653–663
https://doi.org/10.1007/s10895-019-02376-2

ORIGINAL ARTICLE

Synthesis and Computational Studies on Optoelectronically Important Novel Acridin-Isoindoline-1,3-Dione Derivatives

Smita Mane[1] · Kariyappa Katagi[1] · Raveendra Melavanki[2]

Received: 18 September 2018 / Accepted: 3 April 2019 / Published online: 27 April 2019

Abstract
A series of novel 2-(4-(acridin-9-ylamino)phenyl)isoindoline-1,3-dione derivatives were designed and synthesized namely 2-(4-(4-methoxyacridin-9-ylamino)phenyl)isoindoline-1,3-dione [S1], 2-(4-(3-chloroacridin-9ylamino)phenyl)isoindoline-1,3-dione [S2], 2-(4-(2-fluor oacridin-9ylamino)phenyl)isoindoline-1,3-dione [S3], 2-(4-(1,4-dichloroacridin-9ylamino) phenyl)isoindoline-1,3-dione [S4]. The photophysical, thermal properties of these compounds were characterized by the spectroscopic and thermographic method. The absorbance and fluorescence spectra of these derivatives were recorded in different solvents to understand the role of solute and solvent interaction. The compounds showed high thermal stability with thermal decomposition temperatures at 5% weight loss in a range of 250–287 °C. Compared with these compounds, donor groups containing derivatives exhibited excellent properties as fluorescent compounds. Computational studies were done using DFT (Density Functional Theory) G09 software (B3LYP/6-311G++V(d,p)) basis sets in order to calculate the optical band gap and FMO (Frontier Molecular Orbital) energies. The chemical stability of the four derivatives was determined by means of chemical hardness (η) using HOMO-LUMO energies.

Keywords Acridine derivatives · DFT · HOMO-LUMO

Introduction

In this study, four acridin-phthalimide derivatives 2-(4-(4-methoxyacridin-9-ylamino) phenyl)isoindoline-1,3-dione [S1], 2-(4-(3-chloroacridin-9ylamino)phenyl)isoindoline-1,3-dione [S2], 2-(4-(2-fluoroacridin-9ylamino)phenyl)isoindoline-1,3-dione [S3], 2-(4-(1,4-dichloroacridin-9ylamino)phenyl)isoindoline-1,3-dione [S4]. Substituted electron donating and withdrawing groups varying in positions were investigated spectrally in various polar solvents to examine their Solvatochromism luminescent property. As a result, absorbance and fluorescence spectra of the derivative were recorded. Electrochemical properties (HOMO-LUMO) of the acridine derivatives are determined using cyclic voltammetry (CV). DFT is used to calculate HOMO–LUMO energy gap and electrostatic potential map (ESP) of compounds S1-S4. The thermal stability of the derivatives was determined by TGA.

Fluorescence applications have been widely used in material science and biological chemistry because of its selectivity, susceptibility, rapid response, and high spatial resolution via microscopic imaging [1]. The design and synthesis of functional fluorescent dyes have attracted tremendous interest in chemist because of their extensive applications. An ideal fluorescent dye often possesses a high absorption coefficient and quantum yield, a large Stokes shift, high chemical stability, tuneable absorption, and emission profiles and good solubility for practical applications [2].

The effect of solvent on the absorption and fluorescence emission characteristics of organic compounds has been a subject of interesting investigation [3]. Dissolved substances are greatly influenced by solvent parameters like bipolarity, hydrogen bond donating and accepting ability which constitute solute-solvent interactions [4]. The solvatochromic method is based on the shift of absorption and fluorescence maxima in different solvents of varying polarity [5]. Depending on the polarity of the solvent, position, intensity, and shape of the absorption band can vary. Several studies of photophysical properties of organic donor-acceptor molecules suggest intra-molecular charge transfer (ICT) and give access to singlet excited state characteristics, which allows one to design

✉ Kariyappa Katagi
kskatagi69@gmail.com

[1] Department of Chemistry, Karnatak Science College, Dharwad 580001, India

[2] Department of Physics, M S Ramaiah Institute of Technology, Bangalore, Karnataka 560054, India

new molecules and perform in specific applications. These properties include quantum yield, fluorescence decay time, absorption and fluorescence spectral shift [6].

Experimental

Synthesis of 9-Chloroacridine

A mixture of 2-(phenylamino) benzoic acid (0.024 mol) and phosphorus oxychloride (5 mL) was heated on a water bath for 15–20 min. at 80–90 °C and then the reaction mixture was placed in an oil bath at 150 °C for 2 h, the excess of oxychloride was removed by distillation. The cooled reaction mixture was poured in to water and made alkaline with ammonia solution. The product was filtered and washed with hot water [7].

Synthesis of 2-(4-(Acridin-9ylamino) Phenyl) Isoindoline-1, 3-Dione (6a-6j) Derivatives

An equimolar mixture of 9-chloroacridine (0.02 mol) and *p*-phenylene diamine (0.024 mol) was dissolved in 20 mL of methanol and refluxed for 4 h at 70 °C. After the completion of reaction monitored by TLC then it was cooled and poured into diethyl ether the compound starts separation. The product was filtered and recrystallised from ethanol.

The substituted 9-aminoacridine (0.011 mol) and (0.016 mol) pthalic anhydride was refluxed with acetic acid for 5–6 h at 110 °C. The product was filtered and recrystallised. The synthesized compounds S1-S4 outlined in Scheme 1.

Synthesis of 2-(4-(4-Methoxyacridin-9ylamino)Phenyl) Isoindoline-1,3-Dione[S1]

Yield: 75%; dark brown solid; MP =200–202 °C IR (KBr) (Vmax/cm^{-1}): 3340.6, 1716.7, 1635.5, 1532.1 cm^{-1}; ^{1}H NMR (400 MHz, DMSO-d$_6$, δ ppm): 3.56 (s, 3H, -0CH$_3$), 6.44–6.42 (d, 2H, J = 10.4 Hz), 6.89 (s, 1H), 7.39–7.31 (m, 3H), 7.73–7.68 (m, 3H), 8.24–8.22 (d, 2H, J = 6.4 Hz), 8.50–8.39 (m, 4H), 11.55 (s, 1H, -NH); ^{13}C NMR (100 MHz, DMSO, δ ppm): 55.9, 106.8, 107.9, 113.2, 116.4, 116.4, 122.3, 122.4, 122.4, 122.8, 125.4, 127.0, 127.9, 127.9, 128.2, 128.9, 129.9, 132.3, 132.3, 132.6, 132.6, 138.7, 139.5, 148.2, 149.0, 155.8, 167.1, 167.1; GC-MS: m/z 445 (M$^+$).

Synthesis of 2-(4-(3-Chloroacridin-9ylamino)Phenyl) Isoindoline-1,3-Dione[S2]

Yield: 75%; brown solid; MP = 160–162 °C IR (KBr) (Vmax/cm^{-1}): 3444.0, 1721.6, 1629.6, 1524.2 cm^{-1}; ^{1}H NMR (400 MHz, DMSO-d$_6$, δ ppm): 7.20–7.19 (d, 2H, J = 6.4 Hz), 7.48–7.30 (m, 2H), 7.61–7.51 (m, 5H), 7.69–7.67 (d, 2H, J = 7.6 Hz), 7.74 (s, 3H), 8.19–8.14 (m, 1H), 11.47 (s, 1H, -NH); ^{13}C NMR (100 MHz, DMSO, δ ppm): 108.3, 116.5, 116.5, 119.7, 122.4, 122.4, 122.5, 122.8, 127.0, 127.0, 127.6, 127.6, 128.3, 129.0, 129.3, 129.4, 129.9, 132.8, 132.8, 132.9, 134.9, 138.7, 148.2, 149.5, 150.2, 167.1, 167.1; GC-MS: m/z 450 (M$^+$).

Synthesis of 2-(4-(2-Fluoroacridin-9ylamino)Phenyl) Isoindoline-1,3-Dione [S3]

Yield: 70%; brown solid; MP = 208–210 °C IR (KBr) (Vmax/cm^{-1}): 3443.6, 1694.8, 1657.1, 1546.5 cm^{-1}; ^{1}H NMR (400 MHz, DMSO-d$_6$, δ ppm): 6.52–6.50 (d, 2H, J = 8 Hz), 7.44–6.91 (m, 3H), 7.55 (s, 1H), 7.79–7.57 (m, 4H), 8.10–7.89 (m, 5H), 11.36 (s, 1H, -NH); ^{13}C NMR (100 MHz, DMSO, δ ppm): 102.8, 109.2, 116.5, 116.5, 119.6, 122.6, 122.6, 122.6, 122.6, 126.9, 127.0, 127.6, 128.5, 129.0, 129.9, 131.6, 132.2, 132.2, 132.3, 132.3, 138.9, 144.7, 148.4, 149.5, 159.7, 167.6, 167.6; GC-MS: m/z 433 (M$^+$).

Synthesis of 2-(4-(1,4-Dichloroacridin-9ylamino)Phenyl) Isoindoline-1,3-Dione[S4]

Yield: 85%; dark brown solid; MP = 190–192 °C IR (KBr) (Vmax/cm^{-1}): 3445.4, 1742.2, 1622.8, 1516.0 cm^{-1}; ^{1}H NMR (400 MHz, DMSO-d$_6$, δ ppm): 6.44–6.41 (d, 2H, J = 8.8 Hz), 7.41–7.32 (m, 3H), 7.72–7.57 (m, 6H), 8.04 (s, 1H), 8.14–8.12 (d, 2H, J = 8 Hz), 11.36 (s, 1H, -NH);^{13}C NMR

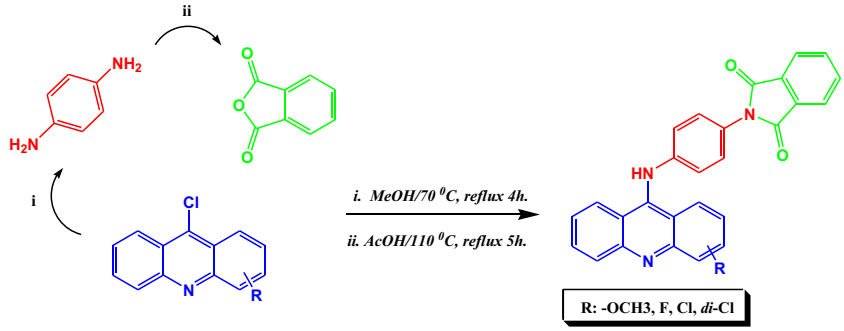

Scheme 1 Synthesis of acridine derivatives S1-S4

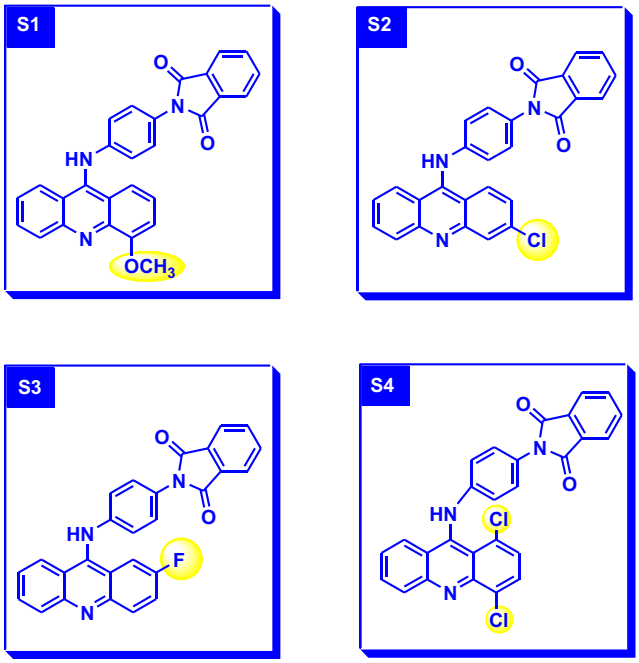

Fig. 1 Molecular structure of acridine derivatives S1, S2, S3 and S4

(100 MHz, DMSO, δ ppm): 111.9, 114.6, 116.4, 116.4, 120.4, 120.4, 122.7, 126.5, 126.9, 127.0, 127.6, 127.6, 128.2, 128.9, 129.8, 130.3, 132.1, 132.1, 132.3, 132.3, 132.6, 138.6, 144.3, 145.6, 153.1, 167.1, 167.1; GC-MS: m/z 484 (M^+).

All the chemicals were purchased from the SD fine and TCI, Mumbai, India. Melting points were determined with an open capillary method on a Buchi apparatus. The IR spectra were recorded on a Nicolet 5700 FT-IR Spectrometer in KBr tablets. ^{1}H and ^{13}C NMR spectra were recorded on Bruker 400 MHz Spectrometer using DMSO-d_6 as solvent and TMS as an internal standard. All chemical shifts were reported as δ values (ppm). Mass spectra were recorded using Shimadzu GCMSQP2010S. The absorption spectra, emission spectra and fluorescence lifetimes were recorded using Carry-100 UV-Visible spectrophotometer, Hitachi F-7000 spectrofluorometer and ISS Chronos BH time-correlated single photon counting (TCS PC) spectrometer respectively. Thermogravimetric Analysis (TGA) and Cyclic Voltammetry (CV) spectra are recorded using SDT Q600 V20.9 Build 20 and Electrochemical analyzer CHI7772C 20 V AC 1.0 A CH Instruments respectively. The DFT method is widely used for finding the energetic and geometric properties of atoms or molecules [8, 9]. In order to determine the HOMO–LUMO energy gap and electrostatic potential map (ESP) of compounds S1-S4. DFT calculations were performed using G09 software (B3LYP/6-311G++V(d, p)) basis sets and using Gaussview 5 visualization program compounds were built and analyzed [10].

Result and Discussion

Synthesis of Acridine Derivatives

9-chloroacridine (1) was prepared according to the literature [7] to this by treatment with a *p*-phenylene diamine to get amine derivatives (2). Further the target compound (3) 2-(4-acridine-9-yl-aminophenyl)isoindoline-1,3-dione was easily achieved by the reaction of N^1-(acridine-9-yl)benzene-1,4-diamine (2) and phthalic anhydride at 110 °C with acetic acid.

Spectroscopic Properties

In order to understand the role of solute-solvent interactions, the effects of solvents on absorption and emission

Table 1 Absorption and Emission data of acridine derivatives in different solvents

Solvents	S1		S2		S3		S4	
	λ^a_{max}	λ^b_{max}	λ^a_{max}	λ^b_{max}	λ^a_{max}	λ^b_{max}	λ^a_{max}	λ^b_{max}
CH	318	432	332	411	338	430	321	397
TL	333	439	332	412	339	438	322	398
BZ	335	443	334	432	339	440	324	421
THF	338	445	336	433	341	447	325	425
BL	339	445	338	435	342	447	325	432
DX	342	446	339	437	344	451	326	435
ML	345	449	340	440	346	451	329	435
AN	346	452	341	443	346	453	330	438
DMF	347	453	341	444	347	455	331	439
DMSO	349	453	342	445	348	456	333	441

Table 2 Optical properties of acridine derivatives S1-S4 in methanol

Compounds	λ^{a}_{max}	λ^{b}_{max}	ϕ_s
S1	345	449	0.56
S2	340	440	0.47
S3	346	451	0.61
S4	329	435	0.66

spectra of each compound were investigated as shown in Fig 1. The absorption and emission spectra of acridine derivatives S1-S4 is carried in ten different polarity solvents such as benzene (BZ), toluene (TL), tetrahydrofuran (THF), butanol (BL), methanol (ML), acetonitrile (AN), N, N-dimethyl formamide (DMF), 1,4-dioxane (DX), cyclohexane (CH), and dimethyl sulphoxide (DMSO) and is listed in Table 1. The absorption bands of compounds S1-S4 in different solvents have shown bathochraomic shift. This may be due to a solvent solute change of the electronic excited state structure in non-polar solvents to polar solvents with increasing solvent polarity. From Table 1 it is observed that emission spectra of compounds in different solvents with varying solvent polarity have shown bathochromic shift (red shift) is due to a π-π* transitions. This may be the indication that substituents are playing a major role in the absorption and emission spectra. Further, on increasing the solvent polarity, the stoke shift value also increases, which may be an indication for intramolecular charge transfer [11]. The Stoke shift (Δλ), indicating the extent of the bathochromic shift of the emission maximum (λ^{emi}_{max}) compared to the absorption maxima (λ^{abs}_{max}), there was a substantial increment in Stoke shift from S1 to S4 as depicted in Table 2.

Figures 2 and 3 shows the absorption and emission spectra of the compounds S1 to S4 along with standard dye POPOP in methanol. From Fig. 2, maximum absorption wavelength bands were observed at 345, 340, 346 and 329 nm for the acridine derivative S1-S4 in methanol respectively. Figure 3, shows the emission maxima for the compounds S1 and S2 at 449 nm and 440 nm whereas, S3 and S4 have shown at 451 nm and 435 nm respectively.

All these absorption spectra (near UV region) were corresponding to the π-π* electron transition [12]. Optical band gaps (E_{opt}) of these compounds were calculated using Eq. (1) from the onset of the low energy side of the absorption spectra (λ) to the baseline and are shown in Table 2.

$$E_{opt} = \frac{1240}{\lambda} \quad (1)$$

From the data it is clear that the band gap goes on increasing from S1-S2, it reveals that the synthesised acridine derivatives can be applicable in organic solar cells (OLEDs) [13].

Quantum Yield

Quantum yield provides important quantum efficiency of the acridine derivatives like excited electronic states, radiationless

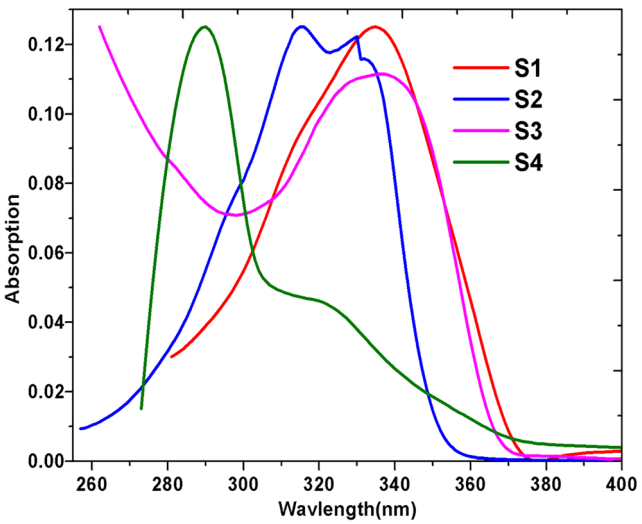

Fig. 2 Absorption spectra of acridine derivative S1-S4

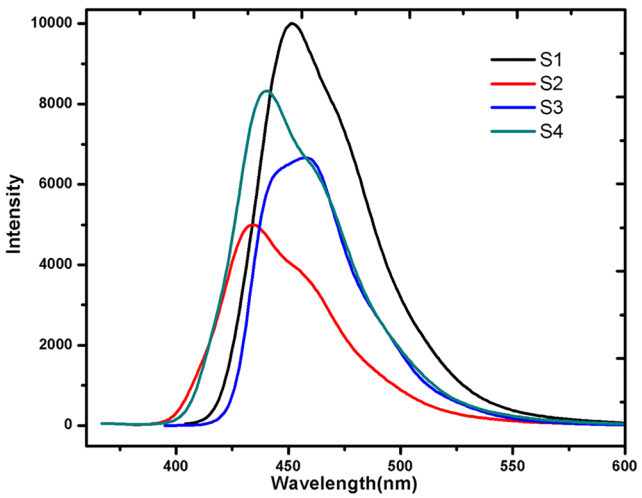

Fig. 3 Emission spectra of acridine derivative S1-S4

transitions, and coupling of electronic to vibronic states. The relative quantum yields (ϕ_s) of acridine derivatives were calculated using comparative method POPOP ($\phi_s = 0.98$) in methanol using as Eq. (2) [14].

$$\Phi_S = \Phi_R \frac{I_S OD_R n_S^2}{I_R OD_S n_R^2} \quad (2)$$

Where I is the intensity of the standard, OD_R is the optical density of the reference, n is the refractive index standard, I_R is the intensity of the reference, n_s is the refractive index of the solvent, OD_S is the optical density of the solvent and n_R is the refractive index of the reference of the fluorophore of known quantum yield. The quantum yields of all the compounds are in the range of 0.47 to 0.66. From Table 2, it is noted that the quantum yield is highest for S4 (0.66) and lowest for S3 (0.47). The quantum yield maxima in case of compound S4 is due to chloro group attached to C1 and C4 position of acridine molecule respectively. Similarly, the quantum yield minima in case of compound S2 is due to fluoro group at the C3 position of the acridine derivatives.

The possible movements of the electron in the acridine are shown in the resonance structure in Fig. 4.

Fluorescence Lifetime

The fluorescence lifetime of the compound S1-S4 was recorded using time-correlated single photon counting technique (TCSPC) in methanol and the average lifetime are given in Table 3. The fluorescence lifetime of all the derivatives are recorded with respect to that of their excitation wavelengths which were obtained from the absorption maxima and each sample was scanned for the 50s. Fluorescence lifetime measurements are the most sensitive measurements to understand the lifetime of the material. Therefore, the decay profile is fitted with tri-exponential function with a χ^2 value close to unity.

$$I = (A_1\tau_1 + A_2\tau_2 + A_3\tau_3) \quad (3)$$

Where τ_1, τ_2, and τ_3 represented the shorter, longer and longest lifetime components with their normalized amplitude components A_1, A_2, and A_3 respectively and lifetime value are given in Table 3. From Table 3 it is observed that the values of χ^2 are close to unity and also these illustrate the accuracy of fluorescence lifetime. Fluorescence lifetime measurement results that compound S1 has higher lifetime 7.88 ns and S2 has the lowest lifetime 6.83 ns.

These may prove that these derivatives are useful for characterization of biological assays such as scanning of tissue surfaces, DNA chip analysis, skin imaging, as well as in optoelectronics like sensors and tuning of dye laser etc.

Determination of HOMO-LUMO Energy States

Cyclic voltammetry (CV) instrument and cyclic voltammogram were used to determine the electrochemical

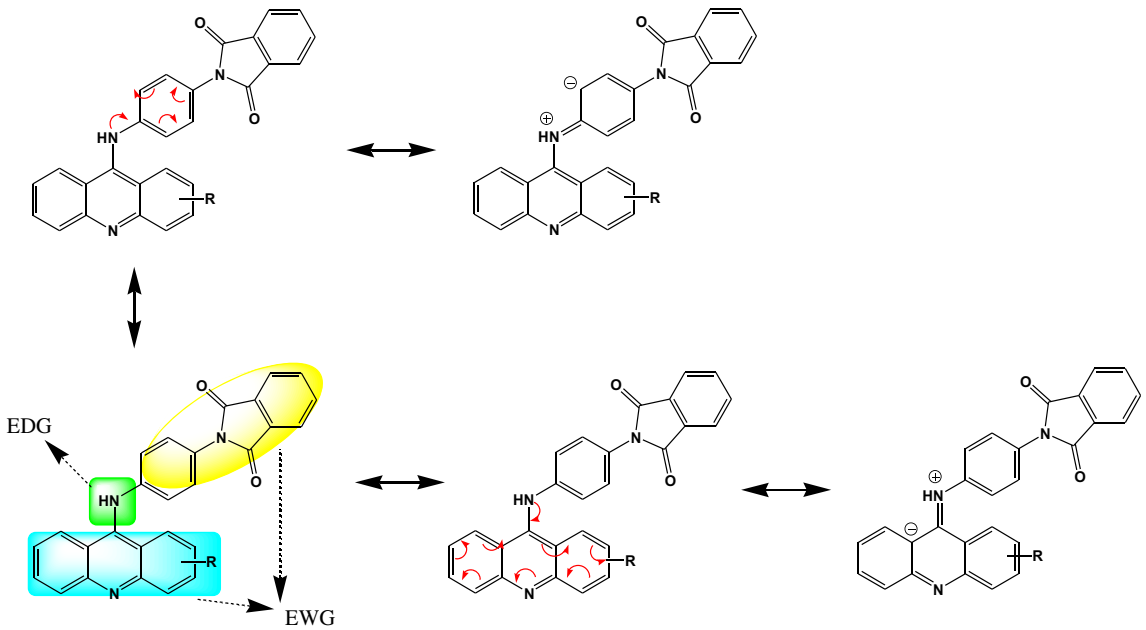

Fig. 4 Possible resonance structure of the S1-S4 acridine derivatives

Table 3 Fluorescence lifetime of acridine derivatives S1-S4 in methanol

Compounds	λ_{exc}	τ_1(ns)	τ_2(ns)	τ_3(ns)	A_1	A_2	A_3	Average lifetime (τ) ns	χ^2
S1	340	0.99	2.54	10.60	0.09	0.19	0.69	7.88	1.06
S2	334	0.48	1.62	8.72	0.09	0.15	0.75	6.83	1.09
S3	342	0.48	2.62	7.90	0.09	0.15	7.90	7.15	1.09
S4	325	0.02	1.57	9.82	0.07	0.17	0.74	7.58	1.07

λ_{exc} – excitation wavelength; τ- average lifetime; A- pre-exponential value; χ- chi square value

properties (HOMO and LUMO) of the acridine derivatives (S1-S4), and are shown in Fig. 5. HOMO (highest occupied molecular orbital) and LUMO (lowest unoccupied molecular orbital) energy levels were calculated by using Eq.4–5 respectively [15] and are given in Table 4.

$$\mathrm{HOMO} = -\left[E_{ox}^{onset} + 4.44\right](\mathrm{eV}) \quad (4)$$

$$\mathrm{LUMO} = \left[\mathrm{HOMO} + E_{opt}\right](\mathrm{eV}) \quad (5)$$

Where,E_{ox}^{onset} is onset oxidation potential and remaining notation have their usual meaning.

The HOMO energy levels of the compounds were determined and found to be in the range of 5.123 to 5.397 eV (vs. Ag/AgCl). From Table 4 it is observed that the values of HOMO increase with the change in a substituent which is attached to the acridine moiety. Lower values of HOMO for compound S1 may be due to the presence of electron donating group (-OCH_3) at the C4 position of acridine ring.

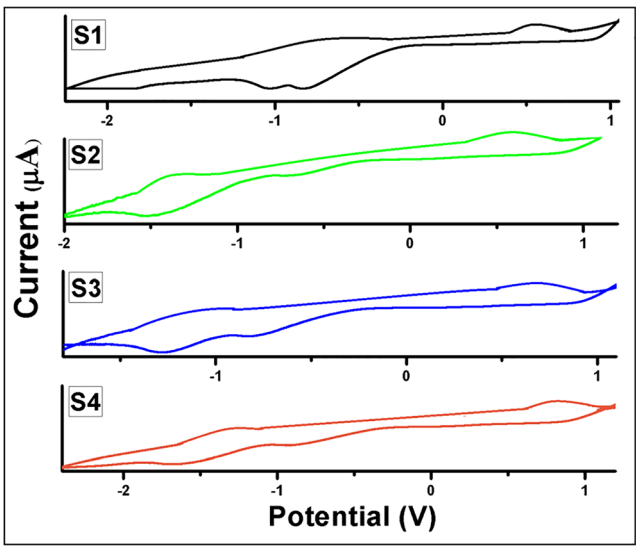

Fig. 5 Cyclic voltammogram curves of compounds S1-S4 were measured in methanol in the presence of nBu_4 NPF_6 at a scan rate of 100 mV s^{-1}

Determination of HOMO-LUMO Energy Gap

Spatial distribution of molecular orbitals, mainly those of HOMO and LUMO are luminous indicators of electron transport in molecular systems [16]. Generally, if the energy gap between the HOMO and LUMO decreases, it is easier for the electrons of the HOMO to be excited. The lowering of the HOMO–LUMO gap is fundamentally a consequence of the large stabilization of the LUMO due to the strong electron-accepting ability of the electron-acceptor group [17].

The difference between HOMO and LUMO energy values gives the HOMO–LUMO energy gap. By using these HOMO–LUMO energy values, the important property like chemical hardness (η) of the chemical compound can be calculated. In the simplest terms, the hardness of a species (atom, ion, or molecule) is a qualitative indication of how polarizable it is, in another way how much its electron cloud is distorted in an electric field. The hardness and softness were suggested in the literature [18–20] to denote resistance to deformation by mechanical force. Molecules with large HOMO–LUMO gap is hard which implies higher stability and opposing charge transfer since they oppose changes in their electron density and distribution. On the contrary, molecules which require a small energy gap for its excitation are also termed as soft molecules. Hence, they are highly polarizable in nature [21].

In terms of chemical change, soft molecules are more reactive than hard molecules. The chemical hardness (η) can be observed by using Eq. (6) [22].

$$\eta = \frac{[E_L - E_H]}{2} \quad (6)$$

Where, E_H is the energy of HOMO and E_L is the energy of LUMO.

The chemical hardness (η) estimated for all the four molecules are given in Table 5. It is observed that chemical hardness is higher for S4 (η =1.4998 eV)

Table 4 HOMO LUMO properties of acridine derivatives S1-S4

Compounds	E_{ox}^{onset} [a]	HOMO[b](eV)	LUMO[c](eV)
S1	0.683	−5.123	−1.793
S2	0.701	−5.141	−1.631
S3	0.824	−5.264	−1.894
S4	0.957	−5.397	−2.177

[a] Oxidation potential relative to Ag/AgCl electrode. [b] Calculated HOMO from the onset oxidation potentials of the compounds using Eq.(4) (eV). [c] Estimated LUMO using empirical Eq.(5)

and least for S1 (η =1.3601 eV). This indicates that the soft molecules require very less energy for excitation. The small difference between η and HOMO-LUMO energy gaps reflects that all molecules under study resulted in soft molecules.

The ground state optimized molecular structures; HOMO and LUMO of all compounds are shown in Fig. 6. The value HOMO, LUMO, and energy band gap (E_g) are given in Table 5. From the Fig. 6 it is observed that the electron clouds of HOMO energy levels are all mainly located on the N^1-(acridine-9yl)benzene-1,4-diamine region of acridine molecules and this data strongly counts for good electron donating property of acridine-diamine unit and LUMO energy levels are mainly concentrated on the (amino-phenyl)isoindoline-1,3-dione unit, except the compound S4. Compared with a all three compounds (S1, S2 and S3) the compound S4 has shown different locality, which is due to the reduction of the energy level of HOMO was higher than that of LUMO because of the introduction of electron withdrawing (Dichloro) group. From the Fig. 7 it is clear that the energy gap between HOMO LUMO is increased in S4. This confirms that introduction of more electron withdrawing group is superior way to increase the energy gap, which is useful in the application of OLEDs due to increase in the enhancement of electron transfer (23). From the Table 5, it is observed that, among the four compounds, S4 which bears the electron-withdrawing dichloro-acridine derivative has shown highest HOMO level compared to others and these results are in good agreement with CV calculations. The partial charge separation of molecules S1-S4 discloses their strong intramolecular charge transfer property, which leads to controllable green color emission. The computationally calculated HOMO energy values are in the range of −5.4141 eV to −5.7660 eV and LUMO energy values are in the range of −2.6938 eV to −2.8196 eV respectively. Optical band gaps obtained from absorption thresholds are in the range of 2.71 to 2.85 eV which are in good agreement with the band gaps 3.22 eV to 3.515 eV obtained using DFT. The energy level diagram of the frontier orbitals is shown in Fig. 7. The presence of strong electron deficient (amino-phenyl)isoindoline-1,3-dione moiety results in the lowering of the LUMO level, which leads to a significant bathochromic shift in the electronic absorption.

To know the reactive sites and hydrogen bonding interaction of the acridine derivatives the electrostatic potential maps (ESP). The MEP of the compound is in use to figure out the reactive sites for electrophilic and nucleophilic attacks and is also useful in biological detection and hydrogen bonding interactions studies [23, 24]. In addition, the MEP is based on the molecular size, shape as well as positive, negative and neutral electrostatic potential region in terms of color grading. The different values of the electrostatic potential at the surface are represented by different colors; red represents regions of most negative electrostatic potential, blue represents regions of most positive electrostatic potential and [25]. It also provides an understanding of the relative polarity of the molecule. The molecular structure with its physicochemical property can be recognized.

Table 5 DFT calculations for the acridine derivatives S1-S4

Compouds	HOMO (eV)	LUMO (eV)	ΔE^a(eV)	E_{opt}(eV)	η
S1	−5.414	−2.693	2.720	3.33 (372 nm)	1.3601
S2	−5. 754	−2.819	2.941	3.51 (353 nm)	1.4705
S3	−5.684	−2.752	2.931	3.37 (367 nm)	1.4658
S4	−5. 766	−2.769	2.999	3.22 (385 nm)	1.4998

ΔE^a - Energy band gap; E_{opt} – optical band gap; η- chemical hardness

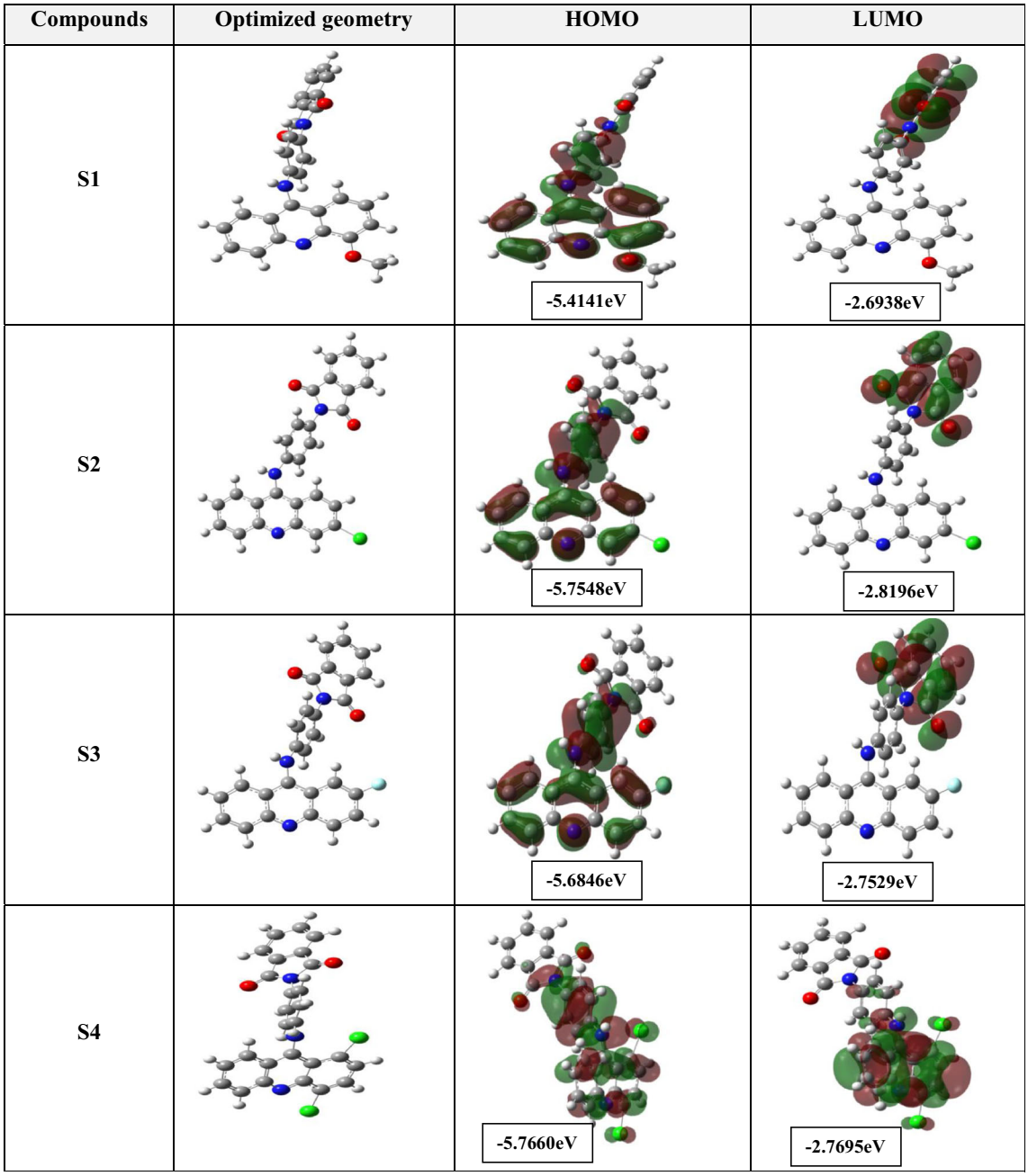

Fig. 6 Molecular orbital amplitude plots of HOMO and LUMO levels and optimized molecular structures of acridine derivative S1-S4 calculated using DFT method

In order to know the charge interrelated properties of the newly synthesised acridine derivative, electrostatic potential maps (ESP) were plotted and are given in Fig. 8. ESP provides visualization of the electron delocalization in a molecule in which acridine derivative shows negative phases around the -OCH_3 which consists of an oxygen molecule at the C4 position of the substituted acridine moiety and a carbonyl group, whereas, positive phases around the nitrogen group present in the acridine-isoindoline moiety and all hydrogen atoms.

Thermogravimetric Analysis (TGA)

The ability of a material to form morphologically stable films is an important requirement for the successful operation of OLEDs. The thermal stabilities of the compounds were studied by thermogravimetric analysis (TGA) under a nitrogen atmosphere, the thermal and morphological stabilities of derivatives of acridine molecules (S1-S4) are summarized Table 6.

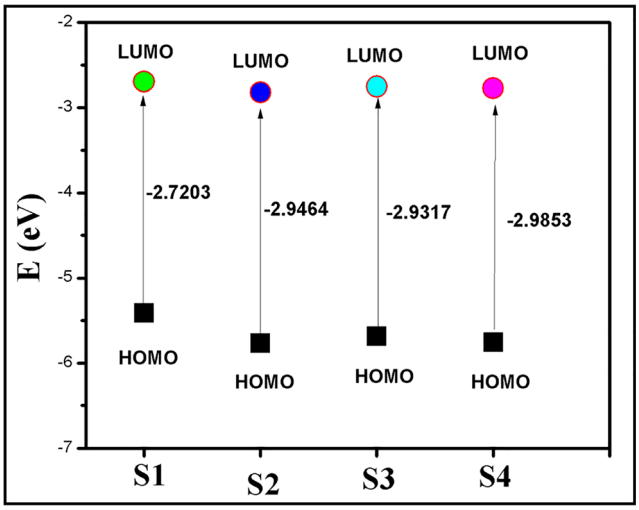

Fig. 7 Energy diagram of the frontier orbitals of acridine derivatives S1-S4 estimated by theoretical (DFT) calculations

Compounds S1-S4 was subjected to thermogravimetric analysis (TGA). The temperatures ranged from room temperature to 400 °C under nitrogen atmosphere (50 mL/min). The TG and Derivative TG grap represented in Fig. 9 and the data are depicted in Table 6. The TGA results reveals that first degradation is observed in all compounds (S1-S4) are in the range of 35–60 °C with minor weight loss (5%) is due to the evaporation of moisture content in the compounds. The major weight loss is observed (S1-S4) in the range of 250–287 °C. It is confirmed that all the compounds shows good thermal stability.

Conclusion

From the above discussion of all the four acridine derivatives, absorption and emission spectra it can be concluded that by increasing the polarity of the solvent, the stoke shift also increases which leads to intramolecular charge transfer. The acridine derivatives S1-S4 have shown bathochromic shift π-π* due to the presence of different substituted electron withdrawing and electron donating groups at a different

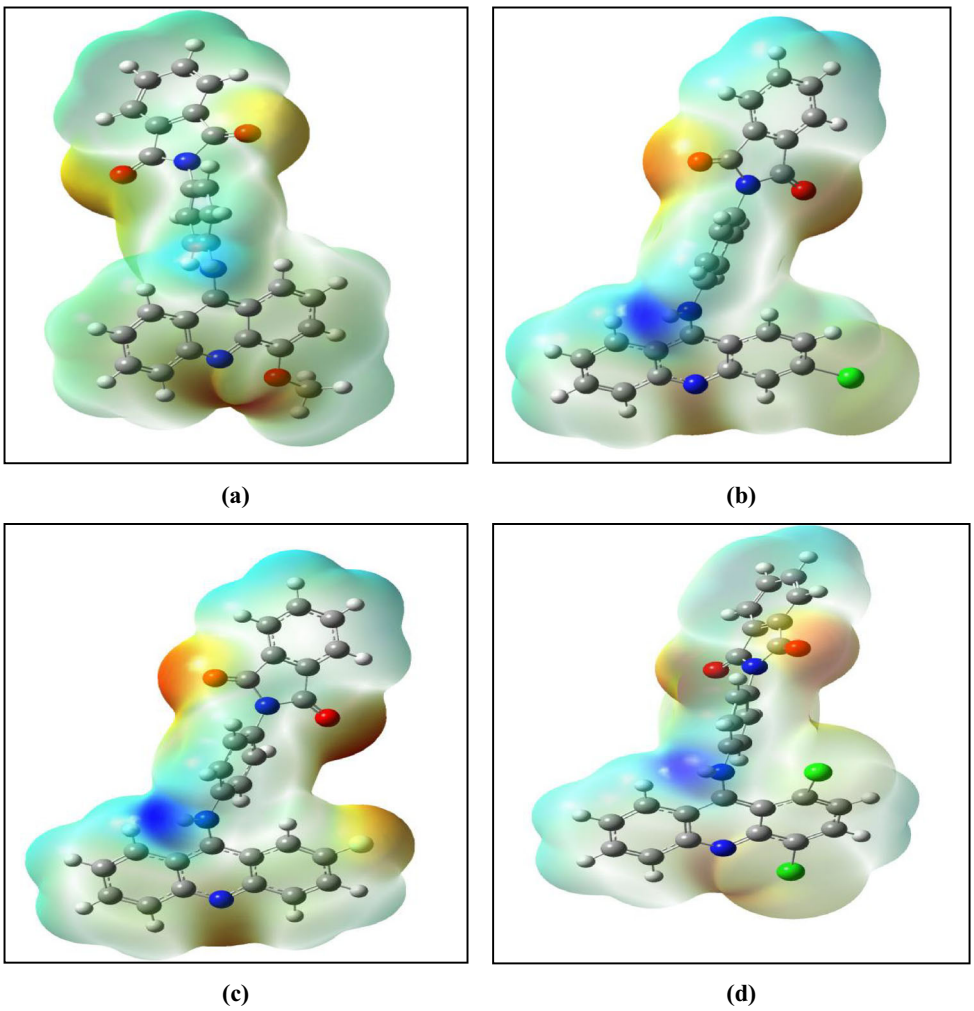

Fig. 8 Molecular electrostatic potential map of acridine derivatives (**a**) S1, (**b**) S2, (**c**) S3 and (**d**) S4

Table 6 Thermal and morphological stabilities of acridine derivatives (S1-S4)

Compounds	I-Degradation % wt loss	II-Degradation % wt loss	III-Degradation % wt loss
S1	41.0 to47.57 °C	–	241.60 to 276.64 °C
	6.70		55.59
S2	36.44 to 39.60 °C	135.87 to 189.48 °C	267 to 286.02 °C
	2.43	5.21	17.50
S3	48.44 to 63.43 °C	170.72 to 194.03 °C	246.68 to 283.25 °C
	6.92	4.96	15.39
S4	39.44 to 42.60 °C	128.58 to 190.33 °C	259 to 287.02 °C
	3.12	4.12	16.78

position of the acridine derivatives. From the fluorescence lifetime, the compound S1 has a higher lifetime (7.88 ns) and S3 has least (6.83 ns) lifetime and hence these may be useful for characterization of the biological assay and can be used in optoelectronics like sensors and OLEDs. From the HOMO-LUMO energy gap, the chemical hardness of the molecules of the acridine derivatives is calculated, which reveal that the compounds are soft in nature due to the presence of small η values. From the TGA studies it can be concluded that all the acridine derivatives are thermally stable.

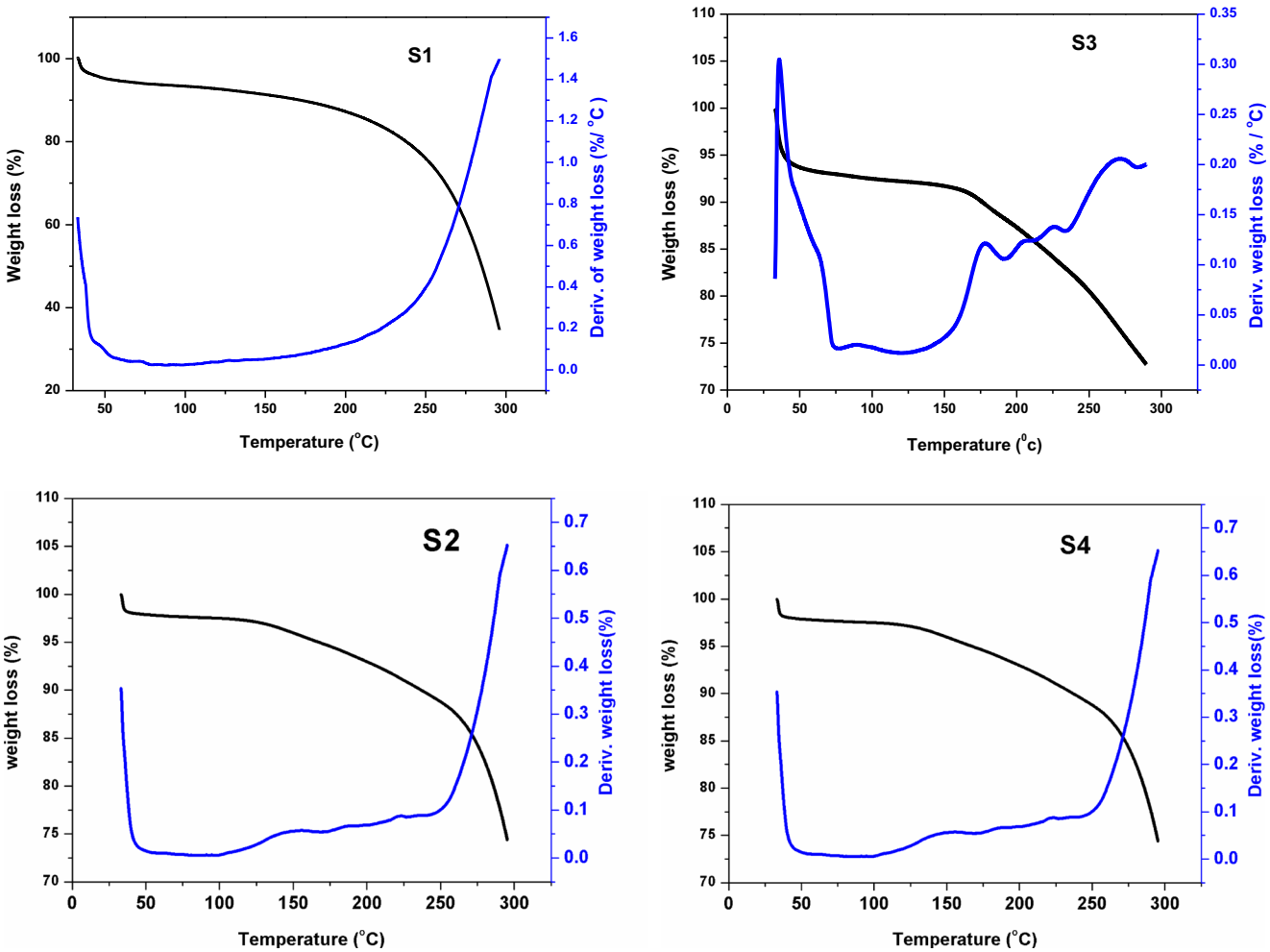

Fig. 9 TGA/Derivative TGA thermograms of the acridine derivatives S1, S2, S3 and S4 measured at a heating rate of 10 °C min^{-1} under Nitrogen atmosphere

Acknowledgments Authors are very much thankful to Department of Chemistry, Karnataka University's Karnataka Science College, Dharwad, for providing necessary Research facilities. Further, Smita. G. Mane and Dr. Kariyappa. S. Katagi highly acknowledges to UGC New Delhi, India for providing Rajiv Gandhi National Fellowship (RGNF) (F117.1/ 2016-17/ RGNF-2015-17-SC-MAH-26074 /(SAIII/Website) and UGC-SWRO, Bangalore for granting research project No. F.2070-MRP/15-16/KAKA056/UGC-SWRO respectively.

References

1. Kumaresan D, Thummel RP, Bura T, Ulrich G, Ziessel R (2009) Colored dual- functional photovoltaic cells. J Eur Chem 15:6335–6339
2. Haugland RP Handbook of Molecular Probes and Research 85 Products (2002) Molecular Probes, OR, 9th edn
3. Melavanki RM, Patil NR, Kapatkar SB, Ayachit NH, Umapathy S, Thipperudrappa J, Nataraju AR (2011) Solvent effect on the spectroscopic properties of 6MAMC and 7MAMC. J MolLiq 158:105–110
4. Benazzouz A, Chebli MM, Hamdi SM, Kheddis BB, Silva AM, Hamdi MJ (2016) Study on Photophysical properties of N-Arylphthalamic acid derivative containing 1, 2, 4-Triazole scaffold. J .Mol.Liq 219:173–179
5. Melavanki RM, Patil HD, Umapathy S, Kadadevarmath JS (2012) Solvatochromic effect on the Photophysical properties of two Coumarins. J Fluoresc 22:137–144
6. Zakerhamidi MS, Sorkhabi SG (2015) Spectral behavior and computational studies of Fuchsin in various solvents. J Lumin 157:220–228
7. Kumar R, Sharma A, Sharma S, Silakari O, Singh M, Kaur M (2013) Synthesis, characterization and antitumor activity of 2-methyl-9-substituted acridines. Arab J Chem 6:79–85
8. Wang X, Xu Y, Yang L, Lu X, Zou H, Yang W, Zhang Y, Li Z, Ma M (2018) Synthesis, spectra, and theoretical investigations of 1,3,5 Triazines compounds as ultraviolet rays absorber based on time-dependent density functional calculations and three-dimensional quantitative structure-property relationship. J Fluoresc 22:12–13
9. Tian J, Yang M, Wang L, Huang X, Feng X, Chu W, Sun ZZ (2016) Synthesis and thermal, electrochemical, photophysical properties of novel symmetric/asymmetric indolo[2,3-a]carbazole derivatives bearing different aryl substituents. Tetrahedron 12:1–9
10. Dennington R, Keith T, Millam J (2009) Semi Chem. Inc., Shawnee Mission GaussView version 5
11. Varma TY, Agarwal DS, Sarmah A, Yukti SR (2016) Photophysical, electrochemical studies of novel Pyrazole-4-yl-2, 3-dihydroquinazolin-4(1H)-ones and their anticancer activity. J Mol Liq 221:1022–1028
12. Roquet S, Cravino A, Leriche P, Aleveque O, Frere P, Roncali J (2006) Triphenylamine-thienylenevinylene hybrid systems with internal charge transfer as donor materials for heterojunction solar cells. J Am Chem Soc 128:3459–3466
13. Marzena GZ, Michal F, Lukasz S, Jacek G, Eric DG, Helmut N, Ewa SB (2012) Thermal, optical, electrochemical, and electrochromic characteristics of novel polyimides bearing the Acridine yellow moiety. Mater Chem Phys 137:221–234
14. Joseph RL (1996) Principles of fluorescence spectroscopy, 3rd edn. Springer, New York
15. Frisch MJ, Trucks GW, Schlegel HB, Scuseria GE, Robb MA, Cheeseman JR, Scalmani G, Barone V (2010) Gaussian-09, Revision B.01, Gaussian, Inc. Wallingford CT
16. Sajan D, Erdogdu Y, Kuruvilla T, Joe IH (2010) Vibrational spectra and first-order molecular hyperpolarizabilities of hydroxybenzaldehyde dimer. J Mol Struct 983:12–21
17. Gázquez JL (1993) Structure and bonding: hardness and softness in DFT theory, vol 80. Springer–Verlag, pp 23–25
18. Pearson RG (1963) Hard and soft acids and bases. J Am Chem Soc 85:3533
19. Pearson RG (1963) Hard and soft acids and bases. Tech and Sci 51: 151 172
20. Shivaram NP, Sanningannavar FM, Navati BS, Patil NR, Kusanur RA, Melavanki RM (2014) Photophysical characteristics of two novel coumarin derivatives: experimental and theoretical estimation of dipole moments using the solvatochromic shift method. Can J Phys 92:1330–1336
21. Muthu S, Prasath M, Paulraj EI, Balaji RA (2014) Spectrochimica Acta part a: molecular and biomolecular spectroscopy FT-IR, FT-Raman spectra and ab initio HF and DFT calculations. Spectrochim Acta Part A Mol Biomol Spectrosc 120:185–194
22. Pearson RG (2005) Chemical Hardnessand density functional theory Wiley – VCH, vol 117, pp 369–377
23. Murray JS, Sen K (1996) Molecular electrostatic potentials, concepts and applications. Chem physics 227:317–329
24. Scrocco E, Tomasi J (1978) Electronic molecular structure, reactivity and intermolecular forces: a heuristic interpretation by means of electrostatic molecular potentials. Adv Quant Chem 11:116–193
25. Thul P, Gupta VP, Ram VJ, Tandon P (2010) Structural and spectroscopic studies on 2-pyranones. Spectrochim Acta A 75:251–260